"Green" electrochemical synthesis of oleic acid modified magnetite nanoparticles

N. Makhaldiani [a], M. Donadze [a,b], L. Targamadze [a], N. Gergauli [a], S. S. Khutsishvili [b,c,*]

[a] *Department of Chemical and Biological Technologies, Georgian Technical University, 77 Kostava St., 0160 Tbilisi, Georgia*

[b] *Rafael Agladze Institute of Inorganic Chemistry and Electrochemistry, Ivane Javakhishvili Tbilisi State University, 11 Mindeli St., 0186 Tbilisi, Georgia*

[c] *School of Medicine, Georgian American University, 10 M. Aleksidze St., 0160 Tbilisi, Georgia*

The research aimed to simplify the electrochemical synthesis of magnetic Fe_3O_4 nanoparticles, and replace it with an eco-friendly process. The new approach involves replacing the two-phase system – water/hexane, used in the synthesis bath of metal-containing nanophase, with single-phase water/ethanol mixture. Using a water/ethanol mixture, the probability of the organic component is significantly reduced. We optimized the synthesis and particles size by variations of electrochemical synthesis conditions. The hybrid nanomagnetite particles were defined using various modern physicochemical methods. The average diameter of nanoparticles is about 3 to 6 nm.

(Received March 14, 2025; Accepted July 24, 2025)

Keywords: Magnetic hybrid nanoparticles, Iron oxide, Fe_3O_4, Oleic acid-shield, Electrochemistry, Metal core-ligand shell

1. Introduction

Magnetic nanoparticles, such as magnetite and maghemite, are less toxic, biocompatible, and magnetically active; therefore, they are widely used in the various biomedical and technical fields [1-4]. For example, magnetic fluids supplied with different stabilizing agents and nanomagnetite or in the form of composites are used in hyperthermia (an alternative way to treat tumor cells), to transfer therapeutic drugs under the action of a magnetic field, as a contrast liquid in magnetic resonance imaging, etc. [5]. In the environmental chemistry, magnetite can purify water and soil from bioorganic pollutants and toxic heavy metals. In the presence of both ions (Fe(II) and Fe(III)), magnetite nanoparticipates in Fenton-like reactions and removes organic pollutants to complete medium purification [6,7]. Therefore, it keeps drawing the scientific community's attention towards designing new materials with magnetite nanoparticles for biomedical applications.

Co-precipitation, hydrothermal, sol-gel, microemulsion, laser pyrolysis, photochemical, ultrasonic, microwave, electrochemical and other methods are used to obtain magnetite nanoparticles [8]. Electrochemical processes are the simplest and environmentally friendly way for obtaining of nanomagnetite. Using electrical energy, electrolyte, and surfactant under appropriate conditions (current density, voltage, temperature); it allows to obtain nanoparticles with controlled shape and size. This process is well described in the literature using different compositions of electrolytes, anode and cathode materials, acidity of the medium, etc. [9-12]. Therefore, to obtain magnetite nanoparticles, we used the electrochemical synthesis method. We demonstrated the success of this approach by obtaining various metal and metal oxide nanoparticles. The nano-sized particles were produced in a galvanic mode, on an arc-shaped rotating cathode in a double-layer bath. Oleic acid (OA), dispersed in hexane or toluene, was used as the organic solvent, and the electrolyte was an aqueous solution containing the corresponding metal ions [13,14]. In this study,

* Corresponding author: khutsishvili_sp@yahoo.com
https://doi.org/10.15251/DJNB.2025.203.859

from the environmental toxicity and economic point of view, the organic solvent (hexane or toluene) was replaced by a water and ethanol mixture.

Electrochemical synthesis mainly occurs in a two-electrode or three-electrode electrochemical cell, in galvanostatic – constant current or potentiostatic – constant potential mode. Other modes – cyclic voltammetry, pulsed potential and current – are often encountered in studies [15]. In galvanostatic mode, the magnetite nanoparticles sizes depend significantly on the current density. As described by Fajarro [16], the particle size (12-25 nm) increases with increasing current density. However, in his study, surfactants were not used in the synthesis, and to prevent aggregation, the current density is usually low and amounts to 100-500 μA/cm2 (0.01-0.05 A/dm2). In Cabrera's publication [17], the electrochemical process occurs at a relatively high current density of 10-200 mA/cm2 (0.1-2 A/dm2), and with increasing current density, the particle size (25-27 nm) does not change significantly. At the cathode, intensive hydrogen reduction occurs, which may be a condition for the formation of magnetite [18].

$$3\gamma - FeOOH + \tfrac{1}{2}H_2 \rightarrow Fe_3O_4 + 2H_2O \quad (1)$$

In an experiment conducted by Lozano [18], because of artificial inflation of hydrogen in the environment of electrochemically formed hydroxide (γ-FeOOH), magnetite was not formed (verified by a diffractometer). It indicates that the hydrogen released at the cathode leaves the reaction zone and does not play a significant part in the formation of magnetite. As can be seen from the study, the diffraction patterns taken from 2 to 90 min confirm the formation of hydroxide γ-FeOOH. At the same time, the magnetite peak formed after 4 min is quite weak, and over time the lepidocrite peak decreases, and after 30 min only the peak characteristic of magnetite remains. Based on the results obtained, authors developed a mechanism for obtaining magnetite by electrolysis:

Anode

$$Fe \rightarrow Fe^{2+} + 2e^- \quad (2)$$

Cathode

$$2H_2O + 2e^- \leftrightarrow H_2 + 2OH^- \quad (3)$$

Oxidation and recombination processes occur in the electrolyte volume

$$Fe^{2+} + 2OH^- \rightarrow Fe(OH)_2 \quad (4)$$

$$3Fe(OH)_2 + \tfrac{1}{2}O_2 \rightarrow 2\gamma FeOOH + Fe(OH)_2 + H_2O \quad (5)$$

$$2\gamma FeOOH + Fe(OH)_2 \rightarrow Fe_3O_4 + 2H_2O \quad (6)$$

Note that since the experiment is conducted in a water-ethanol mixture, ethanol also undergoes oxidation at the anode. Electrochemical synthesis of magnetite in a water-ethanol medium has been described in many papers [9,10].

$$CH_3CH_2OH + \tfrac{1}{2}O_2 \rightarrow 2H^+ + 2e^{-1} + CH_3COOH \quad (7)$$

The electrochemical synthesis of magnetite in a water-ethanol medium was described in many studies, where a solution of iron nitrate and iron chloride was most often used as the electrolyte [9,10,19,20]. In our study, to obtain magnetite nanoparticles, a water/ethanol media in the presence of OA at 55°C, a rotating cathode arc, high current density, and a simple electrolyte were used. Chemical sorption of organic ligand shield (such as OA) gives the excess possibility to avoid nanomagnetites aggregation [21-23]. The manuscript deals with the synthesis of hybrid OA-magnetite nanoparticles and the study of their structure of the obtaining consistent sols of Fe_3O_4-OA [14,24]. These formed OA-magnetite nanosystems show great potential in the design of magnetic fluids, medicines and nanosized sensors, for water treatment, magnetic catalysis, etc. [25,26].

2. Materials and methods

To obtain magnetite nanoparticles, an iron anode (99.19% Fe, 0.75% Mn, 0.053% Cu) and an aluminum cathode-arc, iron sulfate $FeSO_4 \times 7H_2O$ (Sigma-Aldrich, chemical grade), oleic acid (Sigma-Aldrich, chemical grade), deionized water, and ethanol (Khimreactive, 99%) were used.

For electrochemical synthesis, iron sulfate solutions of various concentrations (0.05, 0.8, and 1.0 M) were prepared, as well as a steel cathode (arc) and anode plate. The electrodes were cleaned with sandpaper, degreased with ethanol, washed with double distilled water, dried at 1000°C, and weighed before and after electrolysis. After 30 minutes of electrolysis (the cathode rotation speed of 600 rpm, current density 20-60 A/dm2, temperature 25-55°C), the particles' sizes and zeta potential of the strip, obtained after 10 minutes of centrifugation 8000 rpm, were determined. Based on the theoretically and practically calculated mass of the obtained magnetite, the yield (efficiency) of the process is calculated.

The size of magnetite nanoparticles was determined after each experiment by the dynamic light scattering (DLS) method using Zetasizer-Nano Malvern instrument; before placing the sample in the cuvette, the prepared samples were diluted with ethanol in the ratio 1:8.

The samples for a transmission electron microscopy (TEM) were prepared by depositing small drops of sol onto a carbon-coated copper grid. The prepared samples were examined using a TEM Tesla BS 500.

The Fourier transform infrared (FTIR) spectra were obtained on an Avatar 370 Thermo Nicolet spectrometer with the resolution of 0.5 cm^{-1} (range 400-4000 cm^{-1}) using vaseline. The fine dispersed powder of the obtained sols, after mixing in vaseline oil using an agate stick, was applied to a KB plate.

The Ultraviolet-visible (UV-vis) spectra were recorded on a Varian Cary 100 UV-vis spectrophotometer in the 190-700 nm range. OA dispersed in ethanol was placed in the cuvette of the spectrophotometer, and the test band in the other.

For further experiments, sols with magnetic nanoparticles were washed and heat treated at 300°C (Fig. 1).

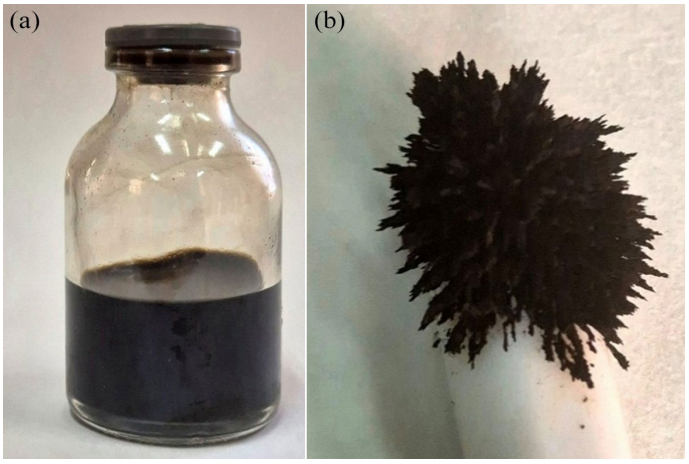

Fig. 1. The obtained OA-magnetite sol (a) and it after heat treatment (b).

Elemental analysis of the obtained powders was determined using the energy-dispersive X-ray spectroscopy function, built into a scanning electron microscope (SEM) JSM-6510LV chamber.

The phase analysis of the powders was established by X-ray diffraction (XRD) using a DRON-4 diffractometer with Cu-Kα radiation.

The simultaneous thermal analysis (thermogravimetric and differential scanning calorimetry (TG-DSC) analysis) was conducted with a NETSCH STA 2500 Regulus synchronous thermal analysis device. The weighed samples (in the form of powders) were heated from 20 to 1000°C at a rate of 10°C per minute. The investigation was done in an oxidizing (air) atmosphere in a corundum crucible for DSC with a height of 6 mm and diameter of 3 mm. The amount of air was sufficient for complete oxidation of the test samples.

For electrochemical studies, a potentiostat-galvanostat IVIUM-Stat with a three-electrode cell was used. A silver chloride electrode Ag/AgCl was used as a reference electrode, a platinum rod was used as an auxiliary electrode. The working electrode was made by mixing 8 mg of nanomagnetite (a sample dried and calcined at 300 °C) with a conducting polymer Poly(3,4-ethylenedioxythiophene) Poly(styrenesulfonate) and drying it at room temperature for 24 h. Polarization curves and cyclic voltammetry were recorded.

3. Results and discussion

Iron sulfate solutions $FeSO_4 \times 7H_2O$ (0.05, 0.8, and 1.0 M) were prepared in various ethanol/water dilutions (50/50, 40/60, 30/70, 20/80, 10/90), and OA was added to each ratio at the following concentrations 0.5, 1.0, and 1.5%. Upon completion of the experiments, we studied the dependence of particles' sizes on current density and electrolysis temperature under all concentration conditions. High current density (60 A/dm2) turned out to be undesirable, since with increasing current density nucleation increases. In addition, this process precedes the stabilization of nanoparticles with OA, which leads to aggregation and enlargement of magnetite nanoparticles. Based on obtained results, following optimal conditions were selected with a water/ethanol ratio 20/80, current density 40 A/dm2, electrolyte $FeSO_4 \times 7H_2O$ 0.05 M, and OA concentration 1.0% at 55°C to inhibit the aggregation of nanoparticles and stabilize them in the sol (Fig. 2).

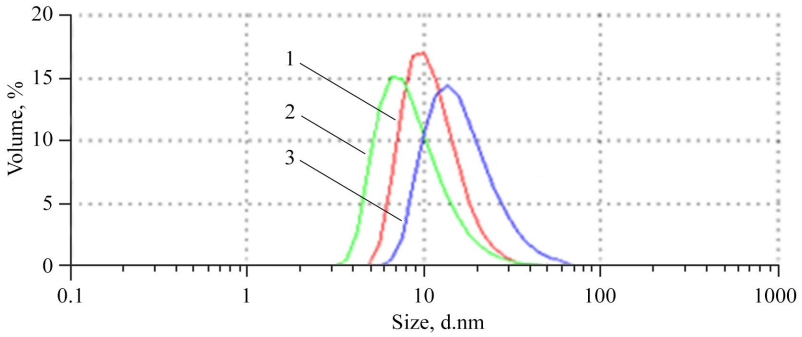

Fig. 2. Magnetite particles' size was estimated using DLS method at different water/ethanol ratios: 1 – 10/90, 2 – 20/80, 3 – 30/70.

In case of excess OA (1.5%), the particles' sizes increase from 8-10 nm to 20-30 nm. It corresponds to our studies of the formation of silver nanoparticles with mono- and bilayer of OA [14]. While a small amount of OA (0.5%) is not enough to stabilize the particles formed; the best results are obtained with OA concentration of 1.0% (Fig. 3).

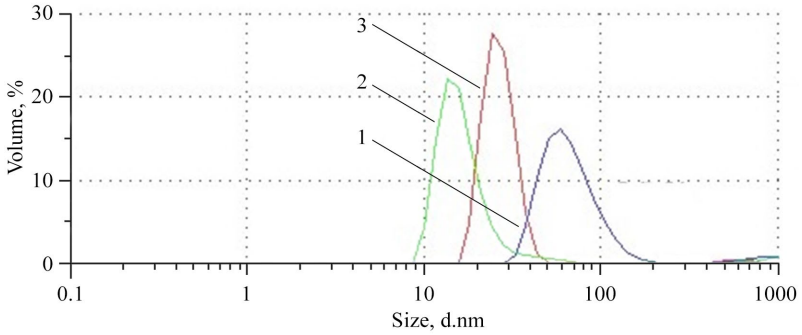

Fig. 3. Magnetite particles' size was estimated using DLS method at water/ethanol ratio 20/80 with different OA concentrations: 1 – 0.5%, 2 – 1.0%, 3 – 1.5%.

TEM micrograph of the OA-magnetite sol shows a uniform distribution of OA-stabilized nanomagnetite in the form of spherical particles (Fig. 4). The sizes of magnetite nanoparticles range in 2-9 nm, with a prevalent size of particles with a diameter of 3-6 nm.

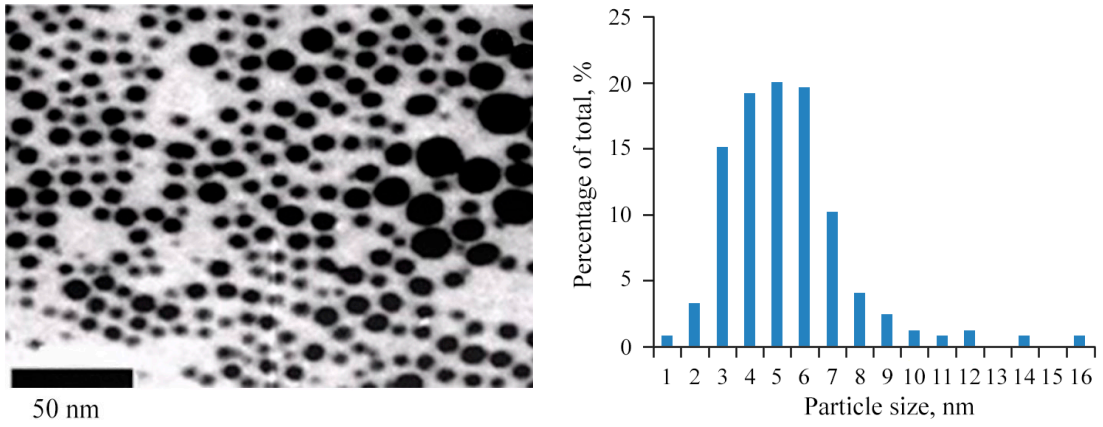

Fig. 4. TEM image and histogram of the size distribution of magnetite nanoparticles capped by OA. The scale bar size is 50 nm.

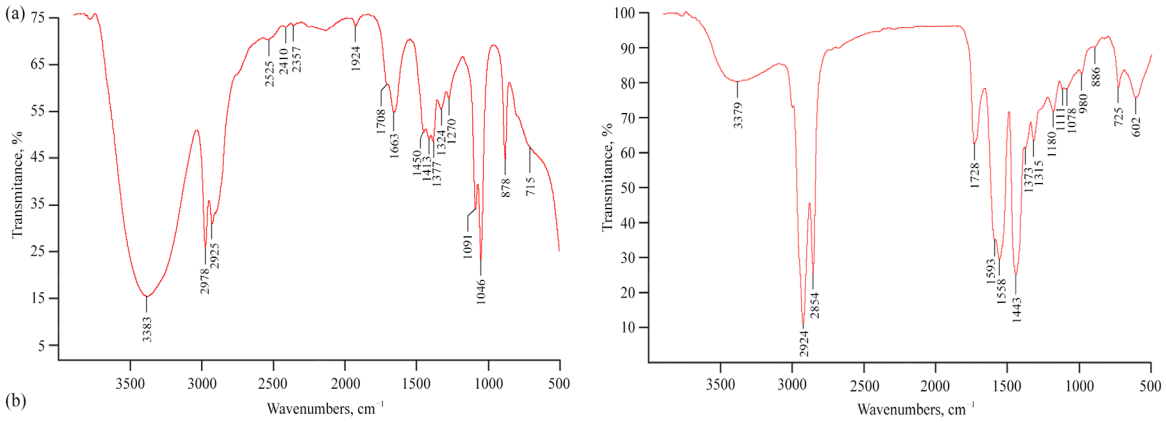

Fig. 5. FTIR spectra of OA dispersed in ethanol (a) and OA-magnetite sol (b).

The FTIR spectrum of OA dispersed in ethanol (Fig. 5a) shows peaks at 2860-2945 cm^{-1} in relation to asymmetric and symmetric vibrations of CH_2 and intensive broad peak at 3383 cm^{-1} for the OH group of ethanol. Characteristic peaks corresponding to C−O (878 cm^{-1}), C−OH (1450 cm^{-1}), C=O (1708 cm^{-1}) are also observed. In the case of OA modified magnetite the peaks characteristic of OA is more pronounced, while the peak characteristic of excess ethanol is no longer visible, see Fig. 5b. The observed spectral characteristics of OA in the presence of magnetite agree with those described in the literature [27]. Thus, peak is observed in the spectrum at 2924 and 2854 cm^{-1} corresponding to the symmetric and asymmetric vibrations of the CH_2 group, the C=O (1728 cm^{-1}), and peaks 1593 and 1558 cm^{-1} correspond to asymmetric and symmetric vibrations of the carboxyl (−COO) group. Additionally, peaks at 602 and 580 cm^{-1} show the characteristic lines of the Fe−O. Newly formed 1078 cm^{-1} vibration is attributed to the chemisorption of Fe_3O_4 with the CO group of OA [11].

To study the thermal stability of the OA-magnetite sol, we used the methods of thermal analysis. Before the experiment, sample was prepared by evaporation at r.t. and dried at 100°C for 3 h to eliminate the aqueous phase. Three main stages of mass reduction are observed on the TG-DSC graphs (Fig. 6). At the first stage of 20-150°C, an endothermic peak is visible at 103°C; in this temperature range, residual moisture is removed and the mass decreases by 10%. At the next stage, a further decrease in mass occurs and an intense exothermic peak is observed at 257°C. It is caused by the active degradation of OA [28], with a mass loss of about 20%. Further mass loss after 300°C that may be the result of magnetite reduction by carbonaceous graphitic residues and gases released during the combustion of OA [28], and other phase processes in the inorganic residue.

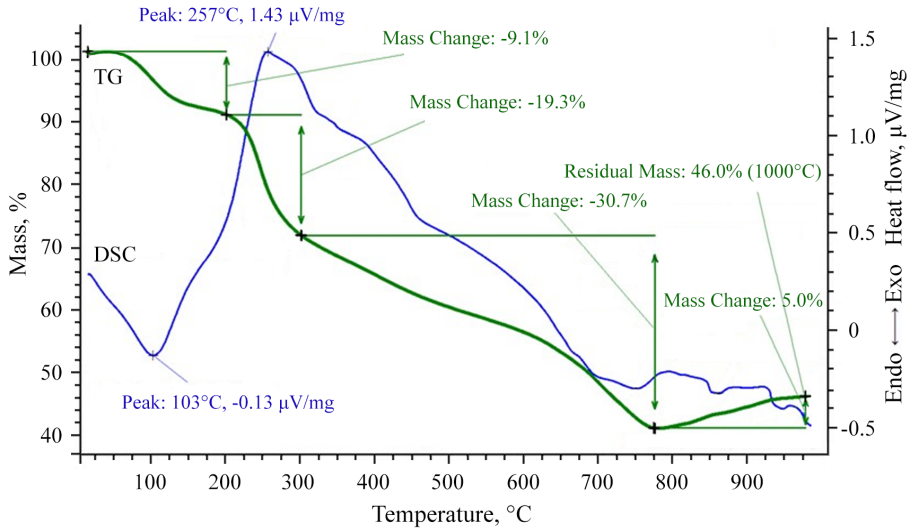

Fig. 6. Thermoanalytical graphics of TG (green) and DSC (blue) of the OA modified nanomagnetite.

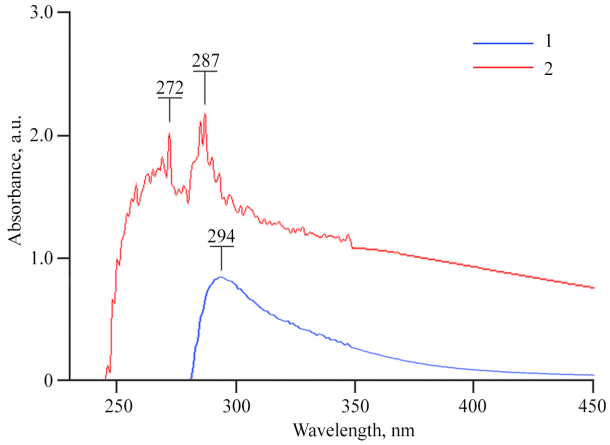

Fig. 7. UV-vis spectra of the OA-ethanol mixture (1), and the OA modified nanomagnetite (2).

In the UV-vis spectrum of the OA modified nanomagnetite, an absorption band corresponding to the magnetite band is observed (272-282 nm), see Fig. 7. The size of the nanoparticle depends on the location of the peak [29]; the closer the peak is to the plasmonic region, the smaller the particle size. The peak of nanomagnetite shifts from the peak corresponding to OA (294 nm) toward the plasmonic region, which indicates the smaller size of magnetite nanoparticles coated with OA [30,31].

Elemental analysis of the nanomagnetite was done by the energy-dispersive X-ray spectroscopy function of a SEM microscope, see Fig. 8a. As can be seen from the analysis, the composition of the obtained substance (Fe – 71.1%, O – 28.9%) corresponds to the magnetite Fe_3O_4 formula. The structure magnetite Fe_3O_4 was characterized using a powder XRD analysis (Fig. 8b). The nucleation of Fe_3O_4 nanocrystals in the OA leads to more broadened diffraction lines (according to the standard) at (2θ) 30.2, 35.6, 43.1, 57.2, and 62.9, characteristic of the face-centered structure of magnetite [32,33].

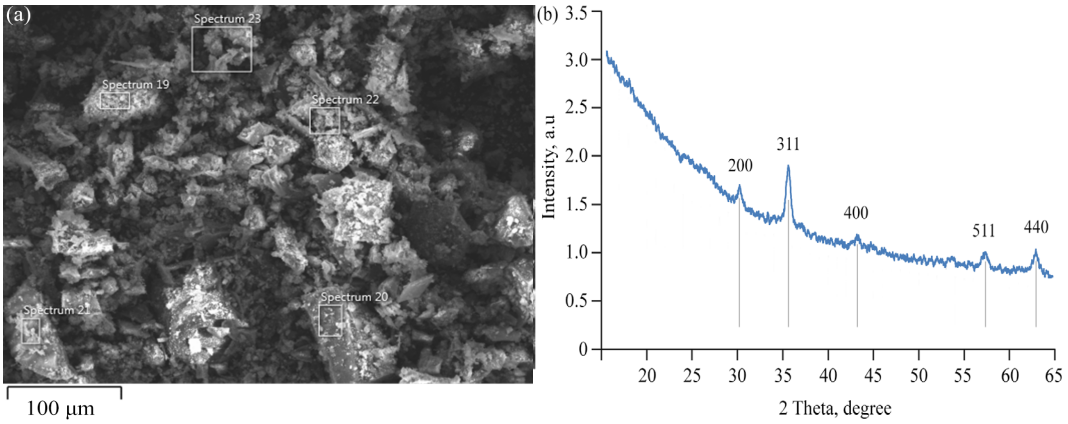

Fig. 8. The SEM image of magnetite nanoparticles (a), and its XRD pattern (b).

According to the results of electrochemical studies, there is practically no difference between the curves (Fig. 9); the steady-state potential in both cases is -0.38 V. The peak is more pronounced in the case of the sample after heat treatment at 300°C, which indicates a decrease in the influence of OA. The electrochemical reactions occurring on top of nanomagnetite were analyzed using voltammetry. In case of nanomagnetite coated with OA, the processes are limited

by the protective layer of OA. While after heat treatment, in the sample two peaks are observed on the cathode curve, indicating a reduction process (Fig. 10).

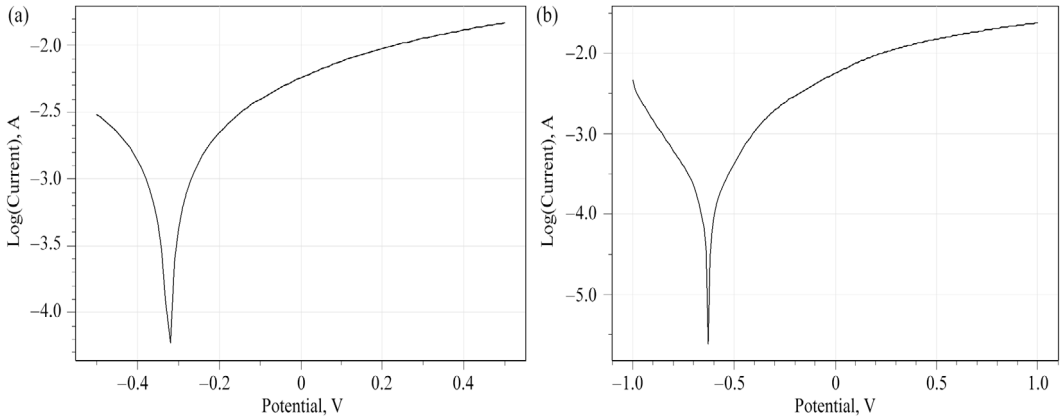

Fig. 9. The polarization curves of the dried nanomagnetite (a), and the calcined sample at 300°C (b).

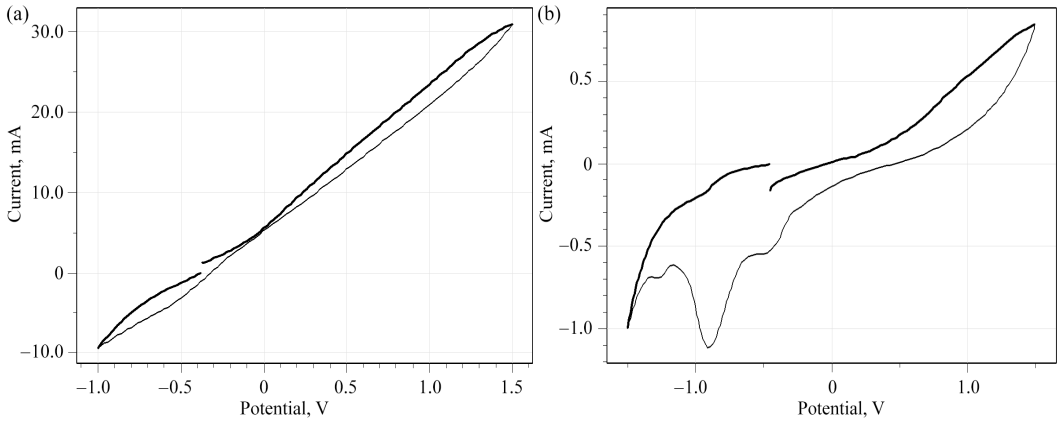

Fig. 10. Voltammetric curves of the dried nanomagnetite (a), and the calcined sample at 300°C (b).

We have demonstrated the success of our proposed a single-phase approach with a water-ethanol mixture for obtaining stable nanomagnetite modified with OA shield under simple eco-friendly conditions. It will reduce costs in the production of such hybrid materials with the possibility of synthetic functionalization of the organic ligand on the magnetite core. Thus, the results obtained open interesting prospects in the design of new magnetic nanomaterials.

4. Conclusions

An electrochemical synthesis method was used to obtain modified nanomagnetite. Replacing the organic solvent (hexane) with a water-ethanol mixture enhanced the process from an ecological and economic point of view, and the optimal settings of the new process were determined. The synthesized nanomagnetite was characterized by instrumental methods, from which replacing hexane with ethanol did not worsen the characteristics of nanomagnetite. Nanoparticles are effectively stabilized by the organic ligand OA. The average diameter of nanoparticles is about 3 to 6 nm, which is confirmed by TEM and DLS measurements. The obtained OA-magnetite sols are promising in the development of new generation hybrid magnetic

nanomaterials for medicine and technology, such as drugs, biosensors, components for microelectronics and in other areas.

Acknowledgements

This work was supported by Shota Rustaveli National Science Foundation of Georgia (SRNSFG) Grant YS-23-511. The authors are grateful to the Center of Instrumental Analysis (Rafael Agladze Institute of Inorganic Chemistry and Electrochemistry, TSU (Tbilisi, Georgia)) for spectral and analytical measurements.

References

[1] K. D. Petrov, A. S. Chubarov, Encyclopedia 2(4), 1811 (2022); https://doi.org/10.3390/encyclopedia2040125

[2] Y. Z. Pan, W. H. Wang, Y. Huang, C. X. Yi, X. Huang, Digest Journal of Nanomaterials and Biostructures 17(1), 137 (2022); https://doi.org/10.15251/DJNB.2022.171.137

[3] A. S. Pozdnyakov, A. A. Ivanova, A. I. Emel'yanov, S. S. Khutsishvili, T. I. Vakul'skaya, T. G. Ermakova, G. F. Prozorova, Russian Chemical Bulletin 66, 2308 (2017); https://doi.org/10.1007/s11172-017-2020-4

[4] Q. Y. Huang, S. Z. Wang, L. Dong, C. Chen, X. L. Zhao, Digest Journal of Nanomaterials and Biostructures 19(1), 435 (2024); https://doi.org/10.15251/DJNB.2024.191.435

[5] M. G. M. Schneider, M. J. Martín, J. Otarola, F. Vakarelska, V. Simeonov, V. Lassalle, M. Nedyalkova, Pharmaceutics 14(1), 204 (2022); https://doi.org/10.3390/pharmaceutics14010204

[6] M. Donadze, N. Makhaldiani, "Electrosinthesis of nanomagnetite and application for purification of phenol previously contaminated water", in: O. Mukbaniani, T. Tatrishvili, M. J. M. Abadie (Eds.), Advanced Polymer Structures, Apple Academic Press, New York, 2023; https://doi.org/10.1201/9781003352181

[7] N. Thomas, D. D. Dionysiou, S. C. Pillai, Journal of Hazardous Materials 404(Part B), 124082 (2021); https://doi.org/10.1016/j.jhazmat.2020.124082

[8] A.-G. Niculescu, C. Chircov, A. M. Grumezescu, Methods 199, 16 (2022); https://doi.org/10.1016/j.ymeth.2021.04.018

[9] R. F. C. Marques, C. Garcia, P. Lecante, S. J. L. Ribeiro, L. Noé, N. J. O. Silva, V. S. Amaral, A. Millán, M. Verelst, Journal of Magnetism and Magnetic Materials 320(19), 2311 (2008); https://doi.org/10.1016/j.jmmm.2008.04.165

[10] I. Karimzadeh, H. R. Dizaji, M. Aghazadeh, Materials Research Express 3, 095022 (2016); https://doi.org/10.1088/2053-1591/3/9/095022

[11] K. Yang, H. Peng, Y. Wen, N. Li, Applied Surface Science 256(10), 3093 (2010); https://doi.org/10.1016/j.apsusc.2009.11.079

[12] N. Rahimdad, A. Khalaj, G. Azarian, D. Nematollahi, Journal of The Electrochemical Society 166, E1 (2019); https://doi.org/10.1149/2.0231902jes

[13] T. Agladze, M. Donadze, M. Gabrichidze, P. Toidze, J. Shengelia, N. Boshkov, N. Tsvetkova, Synthesis and size tuning of metal nanoparticles, Zeitschrift für Physikalische Chemie 227(8), 1187 (2013); https://doi.org/10.1524/zpch.2013.0362

[14] S. S. Khutsishvili, P. Toidze, M. Donadze, M. Gabrichidze, N. Makhaldiani, T. Agladze, Journal of Cluster Science 32, 1351 (2021); https://doi.org/10.1007/s10876-020-01904-6

[15] H. Setyawan, W. Widiastuti, KONA Powder and Particle Journal 36, 145 (2019); https://doi.org/10.14356/kona.2019011

[16] F. Fajaroh, H. Setyawan, W. Widiyastuti, S. Winardi, Advanced Powder Technology 23(3), 328 (2012); https://doi.org/10.1016/j.apt.2011.04.007

[17] L. Cabrera, S. Gutierrez, N. Menendez, M. P. Morales, P. Herrasti, Electrochimica Acta

53(8), 3436 (2008); https://doi.org/10.1016/j.electacta.2007.12.006

[18] I. Lozano, N. Casillas, C. P. de León, F. C. Walsh, P. Herrasti, Journal of The Electrochemical Society 164, 184 (2017); https://doi.org/10.1149/2.1091704jes

[19] M. Ibrahim, K. G. Serrano, L. Noe, C. Garcia, M. Verelst, Electrochimica Acta 55(1), 155 (2009); https://doi.org/10.1016/j.electacta.2009.08.026

[20] M. Starowicz, P. Starowicz, J. Zukrowski, J. Przewoznik, A. Lemanski, C. Kapusta, J. Banas, Journal of Nanoparticle Research 13, 7167 (2011); https://doi.org/10.1007/s11051-011-0631-5

[21] F. C. Carolin, T. Kamalesh, Heliyon 10(9), e29773 (2024); https://doi.org/10.1016/j.heliyon.2024.e29773

[22] G. F. Prozorova, S. A. Korzhova, A. S. Pozdnyakov, A. I. Emel'yanov, S. S. Khutsishvili, T. I. Vakul'skaya, Russian Journal of Applied Chemistry 86, 1452 (2013); https://doi.org/10.1134/S1070427213090230

[23] S. S. Khutsishvili, N. Gagelidze, A. S. Tsokolakyan, M. A. Yeranosyan, E. Tkesheliadze, V. A. Sargsyan, D. Dughashvili, N. Dzebisashvili, K. Aronia, A. Benashvili, D. Dzanashvili, I. Gurgenidze, G. Tatishvili, P. Fraga-García, Materials 18(3), 495 (2025); https://doi.org/10.3390/ma18030495

[24] M. Donadze, M. Gabrichidze, S. Calvache, T. Agladze, The International Journal of Surface Engineering and Coatings 94(1), 16 (2016); https://doi.org/10.1080/00202967.2015.1117263

[25] N.-C. Godja, F.-D. Munteanu, Biosensors 14(2), 67 (2024); https://doi.org/10.3390/bios14020067

[26] N. K. Lotey, S. Pednekar, R. Chaughule, Hybrid nanoparticles in biomedical applications, in: R. S. Chaughule, D. P. Patkar, R. V. Ramanujan (Eds.), Nanomaterials for Cancer Detection Using Imaging Techniques and Their Clinical Applications, Springer, Cham, 2022, pp. 365-400; https://doi.org/10.1007/978-3-031-09636-5_13

[27] J. Ibarra, J. Melendres, M. Almada, M. G. Burboa, P. Taboada, J. Juárez, M. A. Valdez, Materials Research Express 2, 095010 (2015); https://doi.org/10.1088/2053-1591/2/9/095010

[28] O. Bixner, A. Lassenberger, D. Baurecht, E. Reimhult, Langmuir 31(33), 9198 (2015); https://doi.org/10.1021/acs.langmuir.5b01833

[29] S. Baset, H. Akbari, H. Zeynali, M. Shafie, Digest Journal of Nanomaterials and Biostructures 6(2), 709 (2011).

[30] E. Mazario, J. Sánchez-Marcos, N. Menéndez, P. Herrasti, M. García-Hernández, A. Muñoz-Bonilla, RSC Advances 4, 48353 (2014); https://doi.org/10.1039/C4RA08065C

[31] M. Dehghani, B. Hajipour-Verdom, P. Abdolmaleki, Frontiers in Chemistry 12, 1413077 (2024); https://doi.org/10.3389/fchem.2024.1413077

[32] S. A. Medvedeva, G. P. Aleksandrova, L. A. Grishchenko, N. A. Tyukavkina, Russian Journal of General Chemistry 72, 1480 (2002); https://doi.org/10.1023/A:1021654702739

[33] S. S. Khutsishvili, G. P. Aleksandrova, T. I. Vakul'skaya, B. G. Sukhov, IEEE Transactions on Magnetics 57(10), 5200309 (2021); https://doi.org/10.1109/TMAG.2021.3101904